

# 1 **Advances in CLIP technologies for studies of protein-RNA interactions**

2

3 **Flora C. Y. Lee<sup>1,2</sup>, Jernej Ule<sup>1,2,3</sup>**

4 <sup>1</sup> Department of Molecular Neuroscience, UCL Institute of Neurology, Queen Square, London,  
5 WC1N 3BG, UK

6 <sup>2</sup> The Francis Crick Institute, 1 Midland Road, London, NW1 1AT, UK

7 <sup>3</sup> Lead contact: [jernej.ule@crick.ac.uk](mailto:jernej.ule@crick.ac.uk)

## 8 **Summary**

9 RNA binding proteins (RBPs) regulate all aspects in the life cycle of RNA molecules. To  
10 elucidate the elements that guide RNA specificity, regulatory mechanisms and functions of  
11 RBPs, methods that identify direct endogenous protein-RNA interactions are particularly  
12 valuable. UV Crosslinking and Immunoprecipitation (CLIP) purifies short RNA fragments that  
13 crosslink to a specific protein, and then identifies these fragments by sequencing. When  
14 combined with high-throughput sequencing, CLIP can produce transcriptome-wide maps of  
15 RNA crosslink sites. The protocol is comprised of several dozen biochemical steps, and  
16 improvements made over the last 15 years have increased its resolution, sensitivity and  
17 convenience. Adaptations of CLIP are also emerging in the epitranscriptomic field to map the  
18 positions of RNA modifications accurately. Here, we describe the rationale for each step in the  
19 protocol and discuss the impact of variations to help users determine the most suitable option.

## 20 Main Text

### 21 *Introduction*

22 RNA binding proteins (RBPs) play a role in diverse mechanisms of RNA regulation, from pre-  
23 mRNA splicing and 3' end processing to RNA modification, translation, stability and  
24 localisation. Most RBPs are localised at specific cellular locations, where they are presented  
25 with a unique composition of potential RNA targets and other RBPs that affect the binding  
26 patterns through competitive or cooperative interactions. Over a thousand human proteins  
27 have been shown to crosslink to RNA by mass spectrometry studies, including RNA enzymes,  
28 and proteins that lack canonical RNA-binding domains (Baltz et al., 2012; Castello et al.,  
29 2012). In order to disentangle the diverse roles of these proteins, it is necessary to map their  
30 *in vivo* binding sites across the transcriptome.

31 Several methods can be used to identify the endogenous protein-RNA interactions with  
32 variable specificity and sensitivity. The first method developed for this purpose used antibodies  
33 against the spliceosomal Sm proteins (lupus autoimmune sera) to identify the small nuclear  
34 RNAs, which interact with Sm proteins within the abundant spliceosomal small nuclear  
35 ribonucleoproteins (Lerner and Steitz, 1979). This method, later referred to as RIP (for  
36 RNP/RNA immunoprecipitation), relies on immunoprecipitation (IP) of an RBP under  
37 conditions that preserve ribonucleoprotein complexes (RNPs) (Niranjanakumari et al., 2002).  
38 RNPs are preserved either due to mild washing conditions during IP, or by exposing cells to  
39 formaldehyde, which crosslinks protein-protein and protein-RNA interactions. Subsequent  
40 studies used microarrays for transcriptomic analysis of the purified RNAs, and the resulting  
41 method has been referred to as RIP-chip (Keene et al., 2006; Tenenbaum et al., 2000). In  
42 2010, RIP was combined with high-throughput sequencing, and termed RIP-seq (Zhao et al.,  
43 2010). While RIP can identify abundant RNAs bound by an RNP, it is not well suited to studies  
44 of direct protein-RNA contacts. This is because it preserves protein-protein interactions, and  
45 thus can purify multiple RBPs in complex with their bound RNAs. Under some conditions it  
46 can also identify interactions that result from *in vitro* re-associations (Mili and Steitz, 2004).  
47 Therefore, methods with increased specificity for direct RNA binding sites are needed,  
48 especially if one wishes to identify binding sites in lowly abundant RNAs.

49 To identify the position of direct protein-RNA interactions, it is crucial to use a method that  
50 preserves endogenous protein-RNA contacts, while ensuring that only a single specific RBP  
51 is purified. Crosslinking and immunoprecipitation (CLIP) was developed for this purpose by  
52 exploiting zero-length covalent protein-RNA crosslinking and RNA fragmentation (Ule et al.,

53 2003). This enables CLIP to purify RNAs bound to a specific RBP under conditions that are  
54 stringent enough to prevent co-purification of additional RBPs or free RNAs. Moreover, since  
55 only the RNA fragments that are crosslinked to the RBP are isolated, CLIP can identify the  
56 position of the direct RNA binding sites.

57 Initially, CLIP relied on Sanger sequencing to identify 340 sequences corresponding to RNA  
58 interactions of splicing factors Nova1 and Nova2 in mouse brain (Ule et al., 2003). 244 of  
59 these sequences were intronic or intergenic, confirming that CLIP is sensitive enough to  
60 efficiently identify binding sites within low-abundance RNAs. Abundant RNAs such as rRNAs  
61 were absent, underlining the specificity of the method. Even though the sequences were only  
62 approximately 50nt long, they contained on average four Nova-binding motifs, further  
63 confirming the high specificity of CLIP data. Several of the sequences were located next to  
64 alternative exons that turned out to be regulated by Nova proteins, thus demonstrating the  
65 capacity of CLIP to identify the position of functionally important binding sites.

66 Since the original study, multiple variant protocols have been derived to improve the conditions  
67 of RNA fragmentation, RBP purification and cDNA library preparation (Ule et al., 2005),  
68 establish denaturing conditions for RBP purification (Granneman et al., 2009), employ high-  
69 throughput sequencing (Licatalosi et al., 2008; Yeo et al., 2009), determine the position of  
70 crosslink sites at nucleotide resolution (Hafner et al., 2010; König et al., 2010), and increase  
71 the efficiency and convenience of the protocol (Table 1, Table 2). Since RIP or ChIP were  
72 originally combined with microarray readout, the addition of '-seq' (e.g. RIP-seq) was needed  
73 to specify the use of sequencing as opposed to of microarrays. In contrast, the original CLIP  
74 and all the derived variants rely on sequencing. We therefore use the term 'CLIP' to refer  
75 generically to all protocols that purify covalently crosslinked protein-RNA complexes and then  
76 sequence the bound RNA fragments.

77 We describe the core steps of CLIP, the rationale behind each available variation, and their  
78 likely effects on the sensitivity, resolution, specificity or convenience of different protocols (Fig.  
79 1, Table 2). For comparative purpose, we also provide an overview of the steps that are  
80 employed by each of the 28 published protocols (Table S1). We outline the basic approaches  
81 to assess the sensitivity and specificity of CLIP data, while a comprehensive summary of  
82 computational methods for CLIP data analysis is reviewed in more detail elsewhere  
83 (Chakrabarti et al., 2017). We conclude with a discussion of the quality control analyses, and  
84 of the opportunities to apply CLIP to new purposes.

85 *Core steps of CLIP*

86 Although most steps of CLIP have undergone several variations, the core concepts behind  
87 each of the steps and the order of the steps remain largely the same (Fig. 1, Table 1, Table  
88 2). The variants either modify the way the steps are performed, add or omit some of the steps,  
89 in order to increase the efficiency or convenience of the protocol. A central aspect of the  
90 experimental design common to all protocols is the use of appropriate negative controls, which  
91 is important for interpreting the specificity of the purification procedure. The ideal control is to  
92 perform the same purification from cells where the RBP is absent, such as knockout cells, or  
93 when using tag-based purification, cells that do not express a tagged protein (Huppertz et al.,  
94 2014; Ule et al., 2005). As an alternative, non-specific serum or IgG can be used for IP. It is  
95 also valuable to immunoprecipitate the RBP from non-crosslinked cells. If CLIP conditions are  
96 well optimised, these controls should not produce any clearly detectable signal during SDS-  
97 PAGE analysis, and sequencing of their libraries should result in at least 100-fold fewer unique  
98 cDNAs compared to the specific experiments (König et al., 2010).

#### 99 *Covalent crosslinking of protein-RNA contacts*

100 Most variants of CLIP exploit the capacity of ultraviolet (UV) light to promote formation of  
101 covalent bonds between RBPs and their direct RNA binding sites (Table S1). Unlike the  
102 formaldehyde crosslinking that is used in chromatin immunoprecipitation (ChIP) and some  
103 variants of RIP, UV does not crosslink proteins to each other. UV crosslinking requires direct  
104 contact between an amino acid and a nucleobase, and therefore ensures that only direct  
105 protein-RNA interactions are preserved, and the high strength of the covalent bond allows  
106 further stringent purification of individual RBPs and their crosslinked RNA fragments.

107 The original and most later variants of CLIP exposes cells or triturated tissues to the UV-C  
108 wavelength (254nm), which can crosslink RBPs to their bound RNAs without the need for any  
109 additional pre-treatment (Ule et al., 2003). Cells are placed on ice during the short period of  
110 crosslinking in order to avoid any cellular responses, for instance the induction of UV-induced  
111 DNA damage response. The recommended crosslinking procedure for cells in a monolayer  
112 takes 40 seconds (using an energy of 150mJ/cm<sup>2</sup>) (König et al., 2010); this short period allows  
113 a snapshot of the interactions to be captured, thus enabling CLIP to monitor changes in RNP  
114 assembly that occur upon a response to extracellular signals or other treatments (Schor et al.,  
115 2012). A higher total energy can be employed for tissues or cells in suspension, where multiple  
116 rounds of UV exposure with intermittent mixing are needed in order to obtain evenly-  
117 distributed crosslinking throughout the sample. Some protocols employ high UV-C  
118 crosslinking energies also for cells in a monolayer, since this increases crosslinking efficiency

119 and thus sensitivity of CLIP, but this can also increase a cellular response to UV-induced  
120 damage, and the propensity of multiple RBPs to crosslink on the same RNA fragment, thus  
121 risking co-purification of contaminating RBPs. In cases of proteins that do not crosslink well to  
122 RNA, digestion optimized (DO)-RIP-seq could also be employed to identify fragments of RNAs  
123 that are proximal to the protein of interest (Nicholson et al., 2017).

124 PAR-CLIP introduces a variation in the crosslinking strategy (Hafner et al., 2010) (Table 1).  
125 Cells are pre-incubated with photoactivatable ribonucleosides 4-thiouridine (4SU) or 6-  
126 thioguanosine (6SG), which enable protein-RNA crosslinking to be performed with UV-A  
127 wavelength (365nm). Mass spectroscopy analyses indicate two thirds of RBPs efficiently  
128 crosslink with either the standard UV-C (CL) or with the 365nm (PAR-CL), but twice as many  
129 RBPs (24% of the interactome) were identified only by CL compared with 12% for PAR-CL  
130 (Castello et al., 2012). So far, only one mass spectrometry study has compared the CL and  
131 PAR-CL, and therefore the features of RBPs that confer the differential efficiency of these two  
132 crosslinking methods remain unclear. The use of 4SU or 6SG restricts crosslinking to a single  
133 base, and therefore the crosslinking efficiency might also depend on the proximity of these  
134 bases to the binding site. The PAR-CL protocol is limited to biological systems where the  
135 photoactivatable nucleosides can be efficiently incorporated. Incorporation of 4SU through  
136 liquid culture for *C. elegans* or intraperitoneal injection for mouse has enabled studies in model  
137 organisms, however the incorporation rates are lower than in HEK cells in culture (Jungkamp  
138 et al., 2011; Kim et al., 2014), hence they have drawbacks in sensitivity. Moreover, prolonged  
139 preincubation with 6SG (and to a lesser extent 4SU) could cause cellular toxicity, and therefore  
140 care needs to be taken to monitor the cellular response to these ribonucleosides (Burger et  
141 al., 2013; Huppertz et al., 2014). Application of pulsed 4SU has been used in techniques for  
142 tagging and enriching nascent RNAs for sequencing (Windhager et al., 2012), and this  
143 concept could be combined with CLIP to study the patterns of co-transcriptional RNP  
144 assembly on newly transcribed RNAs.

145 The third approach to crosslinking is introduced by m5C-miCLIP, which exploits a mutant  
146 NSun2 RNA methylase enzyme for transcriptome-wide mapping of 5-methylcytosine (m5C)  
147 modification sites (George et al., 2017; Hussain et al., 2013) (Table 1). This mutant enzyme  
148 is incapable of completing the methylation, and instead covalently attaches to the RNA base  
149 at the site of modification. This approach is combined with iCLIP, which has been developed  
150 to amplify cDNAs that truncate at the crosslink site, thus enabling nucleotide-resolution  
151 mapping of the crosslink sites (König et al., 2010) (Table 1). As expected, the crosslink sites  
152 identified by m5C-miCLIP are enriched in cytosines, rather than uridines that are most  
153 common when using UV-C crosslinking in iCLIP (Sugimoto et al., 2012).

154 Finally, proteins can be crosslinked to RNA with UV light *in vitro*. This has been exploited by  
155 variant protocols aimed at studies of RNA methylation, such as m6A-miCLIP (Chen et al.,  
156 2015; George et al., 2017; Ke et al., 2015; Linder et al., 2015) (Table 1). Here, RNA is purified  
157 and partially fragmented, then incubated with an antibody recognising the N6-  
158 Methyladenosine (m6A) modification. Subsequently, UV-C crosslinking is used to form a  
159 covalent bond between the antibody and the modified base. The antibody-RNA complex is  
160 then captured on protein A/G magnetic beads, and the sample continues to the on-bead  
161 adapter ligation and the rest of the iCLIP protocol. Enrichment of the expected sequence motif  
162 at the crosslink sites confirmed the high positional accuracy of the resulting data (Linder et al.,  
163 2015).

#### 164 *Cell lysis*

165 In almost all CLIP derived protocols, a stringent buffer containing ionic detergents is used for  
166 cell lysis, which disrupts most protein-protein and protein-RNA interactions. This increases the  
167 accessibility of RNA and allows unbiased RNase fragmentation, by decreasing the chance  
168 that long RNA binding sites remain protected by large RNPs. It also minimises the chance of  
169 co-purifying multiple associated RBPs during later immunoprecipitation, thus helping to ensure  
170 data specificity.

171 In addition, with methods where the whole cell lysate is used as the input, the proportions of  
172 the different types of RNAs in the resulting data can inform on the cellular distribution of the  
173 RBP. For example, predominance of intronic reads can indicate that the RBP primarily binds  
174 to nascent RNAs on chromatin, whereas enrichment of exonic and junction-spanning reads  
175 indicates that the RBP primarily binds to spliced mRNAs in the cytoplasm. For studies where  
176 the interactome of specific subcellular compartmentalisation is of interest, cell lysis can be  
177 adapted to accommodate the fractionation of sub-cellular compartments. The first protocol  
178 developed for this purpose produced CLIP data from nuclear, cytosolic and polysome fractions  
179 (Sanford et al., 2008). More recently the Fr-iCLIP method has been developed, which  
180 fractionates the nucleus into chromatin and nucleoplasm before proceeding to iCLIP (Brugiolo  
181 et al., 2017) (Table 1).

#### 182 *RNA fragmentation*

183 RNA fragmentation is crucial to avoid co-purifying multiple RBPs that crosslink to the same  
184 RNAs, and to provide insight into the position of RNA binding sites, since the RNA fragment

185 contains the crosslink site. The variation in RNase concentration is unlikely to lead to major  
186 changes in the resulting data, and enriched motifs at the crosslink sites are expected to remain  
187 the same within a range of RNase concentrations (Van Nostrand et al., 2016). However,  
188 analysis of the crosslink sites identified by various PTBP1 iCLIP experiments revealed that  
189 variations in RNase concentrations can lead to changes at the ends of the cDNA inserts, which  
190 correspond to the sites of RNase cleavage (Haberman et al., 2017). Such constraints at the  
191 ends of the cDNA inserts can impact binding site assignment, especially in the case of long  
192 binding sites of RBPs, where appropriate optimisation of RNA fragmentation was found to be  
193 particularly important.

194 Overdigestion results in short RNA fragments, and thus a narrow distribution of cDNA sizes.  
195 This can introduce constraints at the ends of the cDNA insert due to the preferred pattern of  
196 RNase cleavage, and produce short cDNAs that are less likely to map uniquely to the repetitive  
197 regions of the genome (Haberman et al., 2017). On the other hand, insufficient RNA digestion  
198 can lead to co-purification of additional RBPs that bind to the long RNA fragments together  
199 with the immunoprecipitated RBP. This has been exploited in studies which identify RNA-  
200 dependent protein interactors of the RBP-of-interest (Botti et al., 2017; Brannan et al., 2016;  
201 Flury et al., 2014; Klass et al., 2013). Most RNAs contain a large number of binding sites for  
202 many RBPs, hence long RNA fragments could be crosslinked to multiple RBPs at different  
203 positions. Thus, by increasing the presence of co-purified RBPs, long RNA fragments could  
204 decrease the specificity of the final data. An optimal RNA size range of 30-200 nt can be  
205 achieved with a short incubation of the lysate with a low RNase concentration, which can be  
206 optimised by using the visualisation of protein-RNA complexes after SDS-PAGE separation  
207 upon a titration of RNase conditions (Huppertz et al., 2014; Ule et al., 2005). This optimisation  
208 is important especially when starting experiments with a new RBP, or from a new type of cell  
209 or tissue, or when testing new reagent stock.

210 While most protocols perform RNase treatment in the lysate, several protocols employ on-  
211 bead RNase treatment. For example, PAR-CLIP and sCLIP protocols digest with RNase in  
212 the lysate as well as after IP (Hafner et al., 2010; Kargapolova et al., 2017) (Table 1). Zarnegar  
213 and colleagues compared the effects of performing the RNase digestion step either in the  
214 lysate, or on-bead after immunoprecipitation. By using the infrared visualisation in irCLIP  
215 (Table 1), the amount of adapter-ligated RNA-protein complexes can be examined on the  
216 membrane after SDS-PAGE, which showed that the on-bead approach resulted in the highest  
217 signal (Zarnegar et al., 2016). However, it is unclear whether this reflects higher efficiency, or  
218 an increase in non-specific signal. For example, the presence of non-fragmented RNAs during  
219 IP could stabilise large RNPs, leading to formation of multiprotein complexes that would be

220 harder to perturb with later washing steps. While this possibility remains to be examined, the  
221 low density of binding motifs at sites assigned by PTBP1 irCLIP indicates compromised  
222 specificity for this experiment (Haberman et al., 2017).

223 CLIP protocols also differ in the choice of RNase enzymes. The original CLIP used RnaseT1  
224 and RNase A, while the original PAR-CLIP used RnaseT1 and Mnase. These nucleases have  
225 sequence preferences in their cleavage patterns, and extensive digestion can lead to biased  
226 assignment of binding sites from CLIP protocols (Kishore et al., 2011). The iCLIP protocol  
227 introduced the use of RNase I, which is not known to have any nucleotide preferences, and is  
228 thus expected to introduce minimal sequence bias at both ends of RNA fragments (König et  
229 al., 2010). The irCLIP protocol also introduced the use of S1 nuclease, which leaves a 3'OH  
230 instead of a 3' phosphate at the ends of RNA fragments (Zarnegar et al., 2016). This makes  
231 the 3' end dephosphorylation step unnecessary, which otherwise needs to precede the  
232 adapter ligation step. S1 nuclease is a relatively inefficient enzyme on RNA, and therefore we  
233 find its treatment compatible only with the on-bead digestion (data not shown).

234 It is a common misconception that the RNA fragments in CLIP are a signature of RNase  
235 protection. Unlike formaldehyde crosslinking, during which protein-protein interactions are  
236 also crosslinked, UV crosslinking is specific to protein-RNA contacts, and therefore does not  
237 stabilise large RNPs. Instead, CLIP intentionally uses stringent lysis conditions in order to  
238 perturb most native protein-RNA interactions. Thus, the covalent crosslinking normally  
239 remains as the only link between the RBP and the RNA, unless the RBP participates in an  
240 RNP that is unusually stable. If a signature of RNase protection is desired, it would be possible  
241 to lyse the cells under mild conditions that preserve native protein-RNA interactions, perform  
242 RNase fragmentation, and then continue to CLIP with more stringent buffers later during  
243 immunoprecipitation. Alternatively, ribonuclease-mediated protein footprinting methods such  
244 PIP-seq (Silverman et al., 2014) and RIP-iT-Seq (Singh et al., 2014) could be used.

#### 245 *Bead-based purification of the RBP-RNA complex*

246 CLIP allows the purification of RBPs from cells and tissues with stringent immunoprecipitation  
247 conditions, including the use of ionic detergents in the lysis and washing buffers, and the use  
248 of high salt washes. Purification of endogenous RBPs normally requires that antibodies are  
249 available for efficient immunoprecipitation. As an alternative, endogenous RBPs can be  
250 epitope-tagged, which can be achieved with the use of genome editing (Van Nostrand et al.,  
251 2017a). When using epitope-tagging, however, it is important to confirm that the function,  
252 stability and localisation of the tagged RBP remains unperturbed.



253 The need for stringent purification and quality control varies depending on the type and  
254 expression of the RBP being studied. Some RBPs contain many single-stranded RNA binding  
255 domains; for example, ELAVL1 contains three RNA recognition motifs domains, and PTBP1  
256 contains four such domains. These domains recognise U-rich motifs, and are thus expected  
257 to crosslink efficiently. These RBPs are also typically expressed in high abundance. On the  
258 other hand, many RBPs lack canonical binding domains, or recognise the backbone of double-  
259 stranded RNA. It has been shown that cysteine, tryptophan, phenylalanine, tyrosine, arginine,  
260 lysine and methionine are the most reactive (Shetlar et al., 1984), and thus RBPs lacking  
261 these amino acids in close proximity to the RNA base might crosslink poorly. Even a minor  
262 co-purification of another RBP that crosslinks with higher efficiency can lead to major loss of  
263 specificity, and this problem is exacerbated if the RBP-of-interest is of low abundance. Finally,  
264 some RBPs participate in stable RNPs that may not efficiently dissociate under standard CLIP  
265 immunoprecipitation conditions, thus increasing their risk of co-purifying multiple RBPs.

266 In order to minimise the risk of co-purifying multiple RBPs, denaturing strategies are  
267 particularly valuable. Several epitopes enable denaturing and sequential purification  
268 strategies, which can further reduce the chance of co-purifying non-specific RBPs and RNAs.  
269 Denaturing purification was first implemented by CRAC for yeast, and later by CLAP, urea-  
270 iCLIP, uvCLAP and dCLIP (Aktaş et al., 2017; Granneman et al., 2009; Huppertz et al., 2014;  
271 Rosenberg et al., 2017; Wang et al., 2010) (Table 1). Sequential histidine- and streptavidin-  
272 based affinity purification systems are commonly used (Maticzka et al., 2017; Wang et al.,  
273 2010), but immunoprecipitation is also possible if the antibody can bind to the denatured  
274 epitope. An example of an RBP that crosslinks poorly is the double-stranded RNA binding  
275 protein STAU1, which is prone to co-purification with other more abundant and strongly  
276 crosslinking RBPs and the RNAs crosslinked to them. Denaturing purification has been  
277 implemented with a 3xFlag-STAU1 and an anti-Flag antibody by using two rounds of  
278 immunoprecipitation, such that STAU1 was eluted after the first immunoprecipitation with a  
279 high concentration of urea, and then diluted to a lower concentration that enables the second  
280 round of immunoprecipitation (Huppertz et al., 2014).

### 281 *Adapter ligation*

282 To prepare cDNA libraries from the CLIP RNA fragments, they must contain common  
283 sequences complementary to the primers used in reverse transcription (RT) and PCR. Most  
284 CLIP protocols have a similar organisation of the sequenced reads (Fig. 1), therefore we have  
285 named the adapters according to their conventional orientation relative to sequencing. The

286 exceptions are eCLIP and sCLIP (Kargapolova et al., 2017; Van Nostrand et al., 2016), where  
287 the orientation is switched (Table 1). The SeqRv adapter is complementary to the RT primer,  
288 and is ligated to the 3' end of the RNA. The first version of the CLIP protocol ligates the  
289 adapters to purified RNA fragments (Ule et al., 2003), but most later variants perform on-bead  
290 RNA ligation, which reduces the amount of contaminating RNAs (Ule et al., 2005). On-bead  
291 ligation also allows removal of excess adapters by stringent washes of the beads instead of  
292 using denaturing acrylamide gel purification, thus minimising the loss of specific RNAs. An  
293 alternative to the ligation of an adapter to the 3' end of the RNA is developed by sCLIP, where  
294 the purified RNAs are polyadenylated, followed by the use of modified oligo-dT primers for RT  
295 (Kargapolova et al., 2017).

296 The original CLIP protocols ligated both adapters to the RNA fragments, which is also  
297 employed by HITS-CLIP and PAR-CLIP (Table 1, Table 2). This was modified by the iCLIP  
298 protocol, which ligates only the SeqRv adapter to the RNA. The SeqFw adapter, which was  
299 originally ligated to the 5' end of RNA fragments in previous protocols, is introduced to the 5'  
300 end of the RT primer and then brought to the 3' end of the cDNA via circularisation in iCLIP  
301 (König et al., 2010). This enables amplification of cDNAs that prematurely truncate at the  
302 crosslinked nucleotide. These truncated cDNAs lack the SeqFw adapter in the original CLIP  
303 protocols, and are therefore lost. Beyond increasing the sensitivity of the experiment, the  
304 amplification of truncated cDNAs has an additional advantage by enabling nucleotide-  
305 resolution mapping of the crosslink sites, which are located at the start of the great majority of  
306 iCLIP cDNA inserts (Haberman et al., 2017; Sugimoto et al., 2012). Since the development of  
307 iCLIP, 17 other published protocols similarly amplify truncated cDNAs, including BrdU CLIP,  
308 eCLIP, irCLIP and FLASH (Aktaş et al., 2017; Van Nostrand et al., 2016; Weyn-  
309 Vanhentenryck et al., 2014; Zarnegar et al., 2016) (Table 1, Table 2, Table S1). The eCLIP  
310 protocol achieves this by ligating the SeqFw adapter to cDNAs with an intermolecular, rather  
311 than intramolecular ligation.

### 312 *Visualisation of the purified complexes on SDS-PAGE*

313 Visualisation of the protein-RNA complex is the central quality control step in CLIP. It serves  
314 to optimise RNA fragmentation, and to control for the specificity of purified complexes.  
315 Inclusion of this step guarantees the comparative value of CLIP data produced across the  
316 different RBPs, laboratories, and experimental settings. This step purifies the protein-RNA  
317 complexes with the use of SDS-PAGE and membrane transfer. The SDS-PAGE separation  
318 reduces contamination of non-crosslinked RNAs, which normally run at a lower range of the

319 gel than the fragments crosslinked to the RBP. These are further removed by nitrocellulose  
320 membrane transfer, since the membrane has poor RNA-binding capacity. This also helps to  
321 remove excess adapters that can remain stuck on the beads after the RNA ligation step.  
322 Presentation of the resulting images from SDS-PAGE analysis alongside the publication of  
323 data ensures a quality control standard that has been established by the first publication of  
324 CLIP (Ule et al., 2003).

325 In the original protocol, the 5' end of the RNA is radioactively labelled with  $^{32}\text{P}$  in order to  
326 visualize the protein-RNA complexes after transfer to the membrane (Ule et al., 2003). This  
327 serves to control for the specificity of crosslinked RNAs, and to check that the RNA  
328 fragmentation conditions are appropriate (Ule et al., 2005). In certain cases, such as for Ago  
329 HITS-CLIP, where 5' labelling is inefficient, a radiolabeled SeqRv adapter was ligated to the  
330 RNA to enable visualisation (Chi et al., 2009). Two RNA fragmentation conditions are  
331 recommended for the initial experiments. The high RNase condition serves to visualise the  
332 specificity of purified complex, since it migrates as a clear band slightly higher than the  
333 molecular weight (MW) of the immunoprecipitated RBP. To ensure the specificity of CLIP, no  
334 other bands should be visible near the expected band, since these bands indicate co-  
335 purification of non-specific RBPs. The low RNase conditions, in contrast, serves to purify  
336 RNAs for preparation of the cDNA library. This condition should lead to complexes which  
337 migrate diffusely above the apparent MW of the immunoprecipitated RBP, since the diverse  
338 sizes of RNA fragments variably affects the migration of the RBP. The complexes are then  
339 excised from the appropriate region of the membrane according to the described  
340 recommendations (Huppertz et al., 2014; Ule et al., 2005).

341 In the early versions of PAR-CLIP, the membrane transfer step is omitted and the RNA  
342 fragments are purified directly from the SDS-PAGE gel (Hafner et al., 2010). However, the  
343 developers included the option of performing the nitrocellulose membrane transfer in a more  
344 recent PAR-CLIP publication (Garzia et al., 2017). Recently, irCLIP has been developed for  
345 non-radioactive labelling of the purified protein-RNA complexes, increasing the convenience  
346 of this quality control step (Zarnegar et al., 2016). This is achieved by covalently coupling an  
347 infrared dye to the SeqRv adapter, which allows visualisation of the complexes after the SDS-  
348 PAGE and transfer, with infrared imaging which can be performed with a LI-COR Odyssey  
349 CLx Imager. Since the infrared signal is present in the adapter that needs to be ligated to the  
350 RNA fragments, it additionally allows monitoring of on-bead adapter ligation efficiency.  
351 Another strategy for non-radioactive visualisation has been developed in sCLIP, where an  
352 aliquot of the immunoprecipitated sample is labelled with biotin-ADP and RNA ligase. The  
353 labelled and unlabelled fractions then proceed to SDS-PAGE and nitrocellulose transfer,

354 followed by incubation of the membrane with streptavidin-HRP and ECL, in order to visualise  
355 the biotinylated RNA (Kargapolova et al., 2017).

356 Several protocols omit the visualisation of purified complexes. One example is uvCLAP, which  
357 employs denaturing affinity purification, since the additional specificity gained by the  
358 denaturing step reduces the need for further purification by SDS-PAGE (Aktaş et al., 2017).  
359 The FLASH protocol also skips the SDS-PAGE and membrane transfer steps (Aktaş et al.,  
360 2017), but unlike uvCLAP, it does not include denaturing affinity purification, which could  
361 compromise the specificity of data. In eCLIP and seCLIP, the SDS-PAGE and membrane  
362 transfer are used without labelling the RNA, and the RBP-RNA complexes are cut from the  
363 membrane by considering the MW of the RBP as observed on the IP-western performed in  
364 parallel and the predicted shift upwards on the gel due to the crosslinked RNA fragments (Van  
365 Nostrand et al., 2016, 2017b) (Table 1).

366 While increasing the convenience, these protocols risk sacrificing the high specificity of the  
367 method. The specificity of purification conditions can be affected by many factors, including  
368 the cellular material and lysis conditions used, the type of RBP studied, and the stock and  
369 storage time of RNase and other reagents. Maintaining specificity is particularly challenging  
370 for studies of non-canonical RBPs that might crosslink weakly to RNA, or lowly expressed  
371 RBPs, since even a small amount of another co-purified RBP can lead to dominance of its  
372 crosslinked RNAs in the resulting libraries. We therefore advise that the SDS-PAGE  
373 visualisation is used at least initially to optimize the conditions for each RBP, in order to ensure  
374 that complexes are specific and that the RNase fragmentation conditions are appropriate. This  
375 allows the users to be confident in the consistent specificity and comparative value of CLIP  
376 data. When this step is omitted, additional computational quality control steps are crucial in  
377 order to evaluate the specificity of data (Chakrabarti et al., 2017).

### 378 *Reverse transcription (RT)*

379 After visualising the complexes on the nitrocellulose membrane, the appropriate region of the  
380 membrane is excised, and the RBP is digested with proteinase K, which leaves only a short  
381 peptide at the crosslink site and releases the RNA fragments into solution. The resulting RNA  
382 fragments are then available for RT with a primer that contains a sequence complementary to  
383 the SeqRv adapter. In iCLIP, additional sequences have been introduced to the tail of the RT  
384 primer. These include the SeqFw adapter, which is oriented in the opposite direction, an  
385 experimental barcode and the unique molecular identifier (UMI) (Fig. 1). The SeqFw adapter  
386 enables the later intramolecular ligation of the adapter to truncated and readthrough cDNAs;

387 the experimental barcodes enable multiplexing of different cDNA reactions before proceeding  
388 to further steps; and the UMIs (which consist of a sequence of random nucleotides) enable  
389 quantification of unique cDNAs in combination with computational analysis that removes  
390 artefacts of variable PCR amplification (König et al., 2010). UMIs have also been introduced  
391 into the RNA SeqFw adapter in an early HITS-CLIP study (Chi et al., 2009), but explanation  
392 of its use for the analysis of sequencing data was only provided in later publications (Darnell  
393 et al., 2011; Moore et al., 2014).

394 CLIP variants often use different RT enzymes and conditions, including the use of Superscript  
395 II, III or IV, AffinityScript and TGIRT. The impact of different RT conditions on cDNA truncation  
396 and readthrough has been recently investigated (Van Nostrand et al., 2017c). The standard  
397 RT conditions primarily lead to truncation of cDNAs at the crosslinked nucleotide. This feature  
398 of the RT is well exploited by iCLIP and other protocols that ligate SeqFw adapter to cDNAs  
399 after reverse transcription, as they rely on the truncated cDNAs for precise mapping of the  
400 crosslinked nucleotide position. However, use of manganese instead of magnesium ions in  
401 the buffer can increase the efficiency of readthrough, especially when used in combination  
402 with Superscript IV, and this could benefit techniques that rely on readthrough cDNAs, such  
403 as the original CLIP or PAR-CLIP. While most enzymes produce similar cDNA truncation, the  
404 position of truncation may be offset by one nucleotide when AffinityScript (used in eCLIP), is  
405 compared to other enzymes such as Superscript (used in iCLIP and most other protocols)  
406 (Van Nostrand et al., 2017c). This needs to be further examined by comparing the position of  
407 crosslink sites assigned with eCLIP and iCLIP for multiple different RBPs.

#### 408 *cDNA purification and amplification*

409 In the original CLIP or iCLIP protocols, gel purification is used to purify the RNA fragments or  
410 cDNAs, respectively (König et al., 2010; Ule et al., 2003). The primary purpose is to remove  
411 free adapters or RT primers, which would otherwise become templates for reverse  
412 transcription or PCR. Carry-over of excess adapters can lead to cDNA libraries that are  
413 dominated by PCR artefacts which contain only the barcode or adapter sequences. However,  
414 gel purification, phenol-chloroform extractions and ethanol precipitations can be laborious,  
415 especially in large-scale experiments. In recent years, several independent approaches have  
416 been developed to replace the gel purification steps with approaches that increase the  
417 convenience and speed of CLIP protocols, as well as minimising loss of material. These  
418 approaches can be separated conceptually into two types: the first captures nucleic acids  
419 above a certain size range with the use of silica-like beads or columns; the second specifically

420 captures the cDNAs via an incorporated molecule, such as BrdU in BrdU CLIP, or a  
421 biotinylated SeqRv adapter that remains annealed to the cDNA in FAST-iCLIP (Aktaş et al.,  
422 2017; Flynn et al., 2015; Kargapolova et al., 2017; Van Nostrand et al., 2016; Weyn-  
423 Vanhentenryck et al., 2014; Zarnegar et al., 2016) (Table 1, Table 2). It remains to be seen  
424 which of these variant solutions will be most broadly adopted; the ideal solution should be  
425 practical, while efficiently capturing all specific cDNAs without any bias in cDNA size or  
426 sequence, in order to maximize the sensitivity of CLIP.

427 While less convenient, gel extraction provides the most precise size selection of RNA  
428 fragments or cDNAs of defined length, thus mitigating potential variations in cDNA length  
429 distribution in the final library, and ensuring that adapter products are completely removed  
430 prior to PCR. To compensate for this, methods such as FAST-iCLIP and eCLIP that omit gel  
431 extraction before PCR often employ an additional gel extraction of the final PCR-amplified  
432 cDNA libraries (Flynn et al., 2015; Van Nostrand et al., 2016). Loss of material is not a major  
433 concern at this step, since many copies of each cDNA are available due to amplification.  
434 However, this approach could be prone to amplifying adapter artefacts in situations where the  
435 amount of specific cDNA is limiting, for example when studying an RBP that crosslinks poorly.

436 For PCR amplification of cDNAs, most recent methods use enzymes that are slightly more  
437 efficient than the Accuprime enzymes that were used by the original protocols. The switch to  
438 the Phusion enzyme allows amplification of the final cDNA library with a decreased number of  
439 PCR cycles, in our hands, without much impact on the data quality (data not shown). In  
440 general, while a reduced number of PCR cycles required for cDNA amplification is a promising  
441 sign, it should be interpreted cautiously, since it can be due to either an increase in sensitivity  
442 or a decrease in specificity. For example, reduced PCR cycle numbers could arise from the  
443 increased co-purification of non-specific RBPs and their crosslinked RNAs. When the SDS-  
444 PAGE quality control analysis is omitted, one cannot distinguish between these two  
445 possibilities.

#### 446 *Primary data analysis and sequencing requirements*

447 The first step in analysing sequencing data produced by CLIP is to examine the experimental  
448 barcodes to demultiplex the cDNA libraries, which is followed by mapping the data to the  
449 genome. For iCLIP and the 17 later protocols that introduce UMIs into cDNAs (Table 2, Table  
450 S1), this can be used to quantify unique cDNAs that map to same loci on the genome without  
451 ambiguity. The results can then be exploited by using the full position of mapped reads as in  
452 HITS-CLIP (Licatalosi et al., 2008), or by identifying the most likely position of the crosslink

453 site, which can be achieved in three ways. PAR-CLIP examines C to T transitions in reads  
454 (Hafner et al., 2010), iCLIP (and 17 other protocols) examines cDNA truncations (König et al.,  
455 2010), and crosslinking-induced mutation sites (CIMS) in HITS-CLIP reads examines  
456 deletions and other types of mutations (Zhang and Darnell, 2011). Interestingly, analysis of  
457 cDNA truncations was found to be most appropriate for the protocol that crosslinks cells with  
458 4SU as in PAR-CLIP, but then uses iCLIP to prepare the cDNA library (4SU-iCLIP) (Haberman  
459 et al., 2017).

460 Single-end sequencing is appropriate for iCLIP and several derived protocols (such as irCLIP),  
461 because both the experimental barcode and UMI are present at the start of the trimmed  
462 sequencing read (Fig. 1). The start of the cDNA insert contains information for the crosslink  
463 site; the end of the cDNA insert corresponds to the position of RNA cleavage, which is useful  
464 to assess biases of RNA fragmentation (Haberman et al., 2017), but is otherwise not crucial  
465 for data analysis. However, several protocols introduce important information at both sides of  
466 the cDNA inserts, which requires paired-end sequencing, or long-read single-end sequencing  
467 that covers the whole cDNA insert. This applies to eCLIP and sCLIP, where the cDNA insert  
468 is inverted relative to orientation of sequencing; hence the crosslink site needs to be  
469 sequenced from the reverse direction (Kargapolova et al., 2017; Van Nostrand et al., 2016).  
470 uvCLAP and FLASH protocols also use paired-end sequencing, where a part of the  
471 experimental barcode and UMI are introduced by the SeqRv adapter, and are therefore  
472 positioned at the end of the cDNA insert (Aktaş et al., 2017; Garzia et al., 2017). However,  
473 single-end eCLIP (seCLIP) has been recently described, which reverts to the iCLIP-like read  
474 structure compatible with shorter single-end sequencing (Van Nostrand et al., 2017b).  
475 Sequencing of long reads is also beneficial for protocols where the full read or internal  
476 mutations are used for analysis, such as HITS-CLIP and PAR-CLIP, as it allows to fully  
477 quantify the internal mutations in cDNAs.

#### 478 *Analysis of quality and normalisation of CLIP data*

479 In addition to visualising the purified protein-RNA complexes during the CLIP protocol, the  
480 quality of the resulting data can also be examined computationally. Many parameters can be  
481 considered to compare the effectiveness of CLIP-derived methodologies, with sensitivity and  
482 specificity being the two central measures. The simplest measures of sensitivity and specificity  
483 are the number of unique cDNAs in the sequencing library, and clusters of significant  
484 crosslinking events ('peaks'), respectively (Chakrabarti et al., 2017).

485 To monitor the sensitivity of CLIP, the capacity to quantify unique cDNAs with the use of UMIs  
486 is particularly valuable. This is because UMIs distinguish unique cDNAs from those that have  
487 been duplicated as a result of PCR amplification. In addition, the ratio of unique versus  
488 duplicated cDNAs is also a useful measure to assess whether the depth of sequencing was  
489 optimal, and thereby inform on the conditions for most cost-effective sequencing.

490 To monitor the specificity of CLIP, a suitable peak-calling program needs to be chosen  
491 according to the CLIP protocol used to produce the data (Chakrabarti et al., 2017). A low  
492 number of peaks indicates that the cDNAs are randomly dispersed along the transcripts, or  
493 that they are concentrated in a small number of abundant RNAs (such as rRNA). However,  
494 these features could reflect true binding preferences of the RBP that is studied, since many  
495 RBPs don't recognise specific sequence or structural RNA motifs (Jankowsky and Harris,  
496 2015), and therefore the number of crosslink peaks is only a rough approximation of specificity.  
497 For example, proteins such as FUS or SUZ12 have been shown to have low sequence  
498 preference, and therefore their crosslink sites are broadly dispersed across nascent RNAs  
499 (Beltran et al., 2016; Rogelj et al., 2012) and rarely lead to crosslink peaks. Nevertheless,  
500 analysis of crosslink peaks is particularly valuable to compare multiple data sets for the same  
501 RBP. For example, data produced by iCLIP of PTBP1 led to a larger number of peaks than  
502 data produced by other protocols, even though the number of unique cDNAs in iCLIP is equal  
503 or smaller, and this agrees with highest motif enrichment in iCLIP peaks, especially when  
504 compared with irCLIP (Haberman et al., 2017).

505 To normalise the binding patterns relative to RNA abundance, input control libraries that have  
506 not undergone immunoprecipitation can be produced (Ule et al., 2005). Here, the lysate of  
507 crosslinked cells after treatment with RNase is loaded on the gel and transferred to the  
508 membrane. The RNAs that crosslink to all RBPs present in a selected section of the  
509 membrane are isolated and their cDNA library is prepared in the same way as for specific  
510 RBPs. This has been exploited for an approach to analyse eCLIP data, which filters the sites  
511 that are not significantly enriched compared to the size-matched input (SMInput) control (Van  
512 Nostrand et al., 2016, 2017d). This approach can help to enrich the high-affinity binding sites  
513 relative to low-affinity transient interactions, both of which can be detected by CLIP.

514 However, neither definition of crosslink clusters, nor the normalisation by SMInput control can  
515 ensure the specificity of CLIP data. Presence of non-specific RNAs in CLIP is most often  
516 introduced via co-purification of one RBP or a small number of RBPs, along with their  
517 crosslinked RNAs. Since these non-specific RNAs were bound by the co-purified RBPs, they  
518 can lead to the identification of distinct binding peaks that are strongly enriched compared to  
519 the SMInput control, and can have clear motif enrichment. Therefore, the ideal way to validate



520 the specificity of CLIP data is to experimentally visualise the quality of purified RBP-RNA  
521 complexes on SDS-PAGE. Moreover, integrative computational analyses that use orthogonal  
522 functional information can be used, such as comparison with motifs known to be bound by  
523 immunoprecipitated RBP (Haberman et al., 2017). In addition, the metaprofile of binding sites  
524 can be visualised around exons or other RNA landmarks that are regulated by the RBP, and  
525 compared with non-regulated exons, which is commonly referred to as RNA maps. These  
526 approaches, and other methods and databases for computational analysis of CLIP data are  
527 discussed in detail elsewhere (Chakrabarti et al., 2017).

### 528 *Conclusion and future perspectives*

529 The large number and modularity of steps in CLIP provides many opportunities for innovation,  
530 and new purposes to which the method can be applied continue to be discovered. While the  
531 initial development of CLIP was led primarily by the desire for stringent purification and quality  
532 control standards, the more recent methods prioritise speed and convenience. This improves  
533 the capacity for high-throughput studies of many RBPs across many types of conditions,  
534 tissues or species. The use of modified UV illuminators and high-performance UV lasers that  
535 can crosslink proteins to RNA *in vivo* in seconds can also improve the capacity to monitor the  
536 dynamics of protein-RNA complexes at high temporal resolution (van Nues et al., 2017).

537 While these modifications are generally beneficial, common standards for quality control  
538 should be maintained to allow robust comparisons between datasets. We note that current  
539 publically available data from CLIP experiments are generated with protocols that employ  
540 varying stringencies of RBP purification, and depending on the stability of the RNP complexes,  
541 this results in data of variable specificity. Thus, quality measures of specificity will be important  
542 to have a clear interpretation of whether the data represents specific isolation of direct binding  
543 sites for the RBP-of-interest, or rather just an enrichment of such sites (Chakrabarti et al.,  
544 2017). The visualisation of SDS-PAGE-separated protein-RNA complexes and computational  
545 tools for quality analysis of sequenced CLIP libraries will be particularly valuable. Comparison  
546 with methods that do not rely on protein purification or crosslinking to identify RNAs interacting  
547 with RBPs *in vivo*, such as RNA tagging or TRIBE (targets of RNA-binding proteins identified  
548 by editing) (Lapointe et al., 2015; McMahon et al., 2016), could also prove valuable in the  
549 interpretation of CLIP data.

550 In addition to studies of endogenous protein-RNA complexes, variants of CLIP have also been  
551 put to other purposes (Table 1). This includes studies of intermolecular or intramolecular RNA-  
552 RNA contacts (Chi et al., 2009; Imig et al., 2015; Kudla et al., 2011; Sugimoto et al., 2015), as

553 reviewed in more depth elsewhere (Sugimoto et al., 2017). Moreover, CLIP of poly(A)-binding  
554 protein (PABP) can be exploited to study mRNA 3' ends (Hwang et al., 2016); recently, cell-  
555 type specific expression of PABP has been engineered in the mouse brain, thus allowing the  
556 study of cell type specific transcripts (Hwang et al., 2017). Moreover, iCLIP has been adapted  
557 for studies of RNA methylation, as in m5C- and m6A-miCLIP (Hussain et al., 2013; Linder et  
558 al., 2015). These methods could be applied also to other modifications with the use of further  
559 antibodies and mutant enzymes, thus broadening the use of CLIP for the epitranscriptomic  
560 field. Together, the rapidly increasing amount of CLIP data for many RBPs from the ENCODE  
561 consortium and other teams, and the orthogonal methods that interrogate the specificity,  
562 functions and localisation of these RBPs (Van Nostrand et al., 2017d), will enable the study of  
563 how structure and modifications on diverse types of RNAs work together with RBPs to guide  
564 RNP assembly, dynamics and function.

## 565 **Acknowledgements**

566 We wish to thank all members of Ule lab, and in particular Ina Huppertz, Katia Egli, Andrea  
567 Elser, Cristina Militti, Chris Sibley, Kathi Zarnack and Anob Chakrabarti for discussions, critical  
568 reading and feedback on the manuscript. This work was supported by funding from the  
569 European Research Council (617837-Translate) to J.U., a Wellcome Trust Joint Investigator  
570 Award (103760/Z/14/Z) to J.U., a Wellcome Trust Four-Year PhD Studentship  
571 (105202/Z/14/Z) to F.C.Y.L., and the Francis Crick Institute, which receives its core funding  
572 from Cancer Research UK (FC001002), the UK Medical Research Council (FC001002), and  
573 the Wellcome Trust (FC001002).

574 **References**

- 575 Aktaş, T., Avşar Ilık, İ., Maticzka, D., Bhardwaj, V., Pessoa Rodrigues, C., Mittler, G.,  
576 Manke, T., Backofen, R., and Akhtar, A. (2017). DHX9 suppresses RNA processing defects  
577 originating from the Alu invasion of the human genome. *Nature* *544*, 115–119.
- 578 Baltz, A.G., Munschauer, M., Schwanhäusser, B., Vasile, A., Murakawa, Y., Schueler, M.,  
579 Youngs, N., Penfold-Brown, D., Drew, K., Milek, M., et al. (2012). The mRNA-Bound  
580 Proteome and Its Global Occupancy Profile on Protein-Coding Transcripts. *Mol. Cell* *46*,  
581 674–690.
- 582 Beltran, M., Yates, C.M., Skalska, L., Dawson, M., Reis, F.P., Viiri, K., Fisher, C.L., Sibley,  
583 C.R., Foster, B.M., Bartke, T., et al. (2016). The interaction of PRC2 with RNA or chromatin  
584 is mutually antagonistic. *Genome Res.* *26*, 896–907.
- 585 Botti, V., McNicoll, F., Steiner, M.C., Richter, F.M., Solovyeva, A., Wegener, M., Schwich,  
586 O.D., Poser, I., Zarnack, K., Wittig, I., et al. (2017). Cellular differentiation state modulates  
587 the mRNA export activity of SR proteins. *J. Cell Biol.* *216*, 1993–2009.
- 588 Brannan, K.W., Jin, W., Huelga, S.C., Banks, C.A.S., Gilmore, J.M., Florens, L., Washburn,  
589 M.P., Van Nostrand, E.L., Pratt, G.A., Schwinn, M.K., et al. (2016). SONAR Discovers  
590 RNA-Binding Proteins from Analysis of Large-Scale Protein-Protein Interactomes. *Mol. Cell*  
591 *64*, 282–293.
- 592 Brugiolo, M., Botti, V., Liu, N., Müller-McNicoll, M., and Neugebauer, K.M. (2017).  
593 Fractionation iCLIP detects persistent SR protein binding to conserved, retained introns in  
594 chromatin, nucleoplasm and cytoplasm. *Nucleic Acids Res.* *45*, 10452–10465.
- 595 Burger, K., Mühl, B., Kellner, M., Rohrmoser, M., Gruber-Eber, A., Windhager, L., Friedel,  
596 C.C., Dölken, L., and Eick, D. (2013). 4-thiouridine inhibits rRNA synthesis and causes a  
597 nucleolar stress response. *RNA Biol.* *10*, 1623–1630.
- 598 Castello, A., Fischer, B., Eichelbaum, K., Horos, R., Beckmann, B.M., Strein, C., Davey,  
599 N.E., Humphreys, D.T., Preiss, T., Steinmetz, L.M., et al. (2012). Insights into RNA Biology  
600 from an Atlas of Mammalian mRNA-Binding Proteins. *Cell* *149*, 1393–1406.
- 601 Chakrabarti, A.M., Haberman, N., Praznik, A., Luscombe, N.M., and Ule, J. (2017). Data  
602 Science Issues in Understanding Protein-RNA Interactions. *BioRxiv* doi:10.1101/208124.
- 603 Chen, K., Lu, Z., Wang, X., Fu, Y., Luo, G.-Z., Liu, N., Han, D., Dominissini, D., Dai, Q.,  
604 Pan, T., et al. (2015). High-Resolution *N*<sup>6</sup>-Methyladenosine (m<sup>6</sup>A) Map Using Photo-  
605 Crosslinking-Assisted m<sup>6</sup>A Sequencing. *Angew. Chem. Int. Ed.* *54*, 1587–1590.
- 606 Chi, S.W., Zang, J.B., Mele, A., and Darnell, R.B. (2009). Argonaute HITS-CLIP decodes  
607 microRNA–mRNA interaction maps. *Nature* *460*, 479–486.
- 608 Darnell, J.C., Van Driesche, S.J., Zhang, C., Hung, K.Y.S., Mele, A., Fraser, C.E., Stone,  
609 E.F., Chen, C., Fak, J.J., Chi, S.W., et al. (2011). FMRP Stalls Ribosomal Translocation on  
610 mRNAs Linked to Synaptic Function and Autism. *Cell* *146*, 247–261.

- 611 Flury, V., Restuccia, U., Bachi, A., and Mühlemann, O. (2014). Characterization of  
612 Phosphorylation- and RNA-Dependent UPF1 Interactors by Quantitative Proteomics. *J.*  
613 *Proteome Res.* *13*, 3038–3053.
- 614 Flynn, R.A., Martin, L., Spitale, R.C., Do, B.T., Sagan, S.M., Zarnegar, B., Qu, K., Khavari,  
615 P.A., Quake, S.R., Sarnow, P., et al. (2015). Dissecting noncoding and pathogen RNA–  
616 protein interactomes. *RNA* *21*, 135–143.
- 617 Garzia, A., Meyer, C., Morozov, P., Sajek, M., and Tuschl, T. (2017). Optimization of PAR-  
618 CLIP for transcriptome-wide identification of binding sites of RNA-binding proteins.  
619 *Methods San Diego Calif* *118–119*, 24–40.
- 620 George, H., Ule, J., and Hussain, S. (2017). Illustrating the Epitranscriptome at Nucleotide  
621 Resolution Using Methylation-iCLIP (miCLIP). In *RNA Methylation*, (Humana Press, New  
622 York, NY), pp. 91–106.
- 623 Granneman, S., Kudla, G., Petfalski, E., and Tollervey, D. (2009). Identification of protein  
624 binding sites on U3 snoRNA and pre-rRNA by UV cross-linking and high-throughput  
625 analysis of cDNAs. *Proc. Natl. Acad. Sci.* *106*, 9613–9618.
- 626 Haberman, N., Huppertz, I., Attig, J., König, J., Wang, Z., Hauer, C., Hentze, M.W., Kulozik,  
627 A.E., Le Hir, H., Curk, T., et al. (2017). Insights into the design and interpretation of iCLIP  
628 experiments. *Genome Biol.* *18*, 7.
- 629 Hafner, M., Landthaler, M., Burger, L., Khorshid, M., Hausser, J., Berninger, P., Rothballer,  
630 A., Ascano Jr., M., Jungkamp, A.-C., Munschauer, M., et al. (2010). Transcriptome-wide  
631 Identification of RNA-Binding Protein and MicroRNA Target Sites by PAR-CLIP. *Cell* *141*,  
632 129–141.
- 633 Huppertz, I., Attig, J., D’Ambrogio, A., Easton, L.E., Sibley, C.R., Sugimoto, Y., Tajnik, M.,  
634 König, J., and Ule, J. (2014). iCLIP: Protein–RNA interactions at nucleotide resolution.  
635 *Methods San Diego Calif* *65*, 274–287.
- 636 Hussain, S., Sajini, A.A., Blanco, S., Dietmann, S., Lombard, P., Sugimoto, Y., Paramor, M.,  
637 Gleeson, J.G., Odom, D.T., Ule, J., et al. (2013). NSun2-Mediated Cytosine-5 Methylation of  
638 Vault Noncoding RNA Determines Its Processing into Regulatory Small RNAs. *Cell Rep.* *4*,  
639 255–261.
- 640 Hwang, H.-W., Park, C.Y., Goodarzi, H., Fak, J.J., Mele, A., Moore, M.J., Saito, Y., and  
641 Darnell, R.B. (2016). PAPERCLIP Identifies MicroRNA Targets and a Role of CstF64/64tau  
642 in Promoting Non-canonical poly(A) Site Usage. *Cell Rep.* *15*, 423–435.
- 643 Hwang, H.-W., Saito, Y., Park, C.Y., Blachère, N.E., Tajima, Y., Fak, J.J., Zucker-Scharff, I.,  
644 and Darnell, R.B. (2017). cTag-PAPERCLIP Reveals Alternative Polyadenylation Promotes  
645 Cell-Type Specific Protein Diversity and Shifts Araf Isoforms with Microglia Activation.  
646 *Neuron* *95*, 1334–1349.e5.
- 647 Imig, J., Brunschweiler, A., Brümmer, A., Guennewig, B., Mittal, N., Kishore, S., Tsikrika,  
648 P., Gerber, A.P., Zavolan, M., and Hall, J. (2015). miR-CLIP capture of a miRNA targetome  
649 uncovers a lincRNA H19–miR-106a interaction. *Nat. Chem. Biol.* *11*, 107.

650 Jankowsky, E., and Harris, M.E. (2015). Specificity and nonspecificity in RNA-protein  
651 interactions. *Nat. Rev. Mol. Cell Biol.* *16*, 533–544.

652 Jungkamp, A.-C., Stoeckius, M., Mecnas, D., Grün, D., Mastrobuoni, G., Kempa, S., and  
653 Rajewsky, N. (2011). In Vivo and Transcriptome-wide Identification of RNA Binding  
654 Protein Target Sites. *Mol. Cell* *44*, 828–840.

655 Kargapolova, Y., Levin, M., Lackner, K., and Danckwardt, S. (2017). sCLIP—an integrated  
656 platform to study RNA–protein interactomes in biomedical research: identification of  
657 CSTF2tau in alternative processing of small nuclear RNAs. *Nucleic Acids Res.* *45*, 6074–  
658 6086.

659 Ke, S., Alemu, E.A., Mertens, C., Gantman, E.C., Fak, J.J., Mele, A., Haripal, B., Zucker-  
660 Scharff, I., Moore, M.J., Park, C.Y., et al. (2015). A majority of m6A residues are in the last  
661 exons, allowing the potential for 3' UTR regulation. *Genes Dev.* *29*, 2037–2053.

662 Keene, J.D., Komisarow, J.M., and Friedersdorf, M.B. (2006). RIP-Chip: the isolation and  
663 identification of mRNAs, microRNAs and protein components of ribonucleoprotein  
664 complexes from cell extracts : Article : Nature Protocols. *Nat Protoc.* *1*, 302–307.

665 Kim, K.K., Yang, Y., Zhu, J., Adelstein, R.S., and Kawamoto, S. (2014). Rbfox3 controls the  
666 biogenesis of a subset of microRNAs. *Nat. Struct. Mol. Biol.* *21*, 901.

667 Kishore, S., Jaskiewicz, L., Burger, L., Hausser, J., Khorshid, M., and Zavolan, M. (2011). A  
668 quantitative analysis of CLIP methods for identifying binding sites of RNA-binding proteins.  
669 *Nat. Methods* *8*, 559–564.

670 Klass, D.M., Scheibe, M., Butter, F., Hogan, G.J., Mann, M., and Brown, P.O. (2013).  
671 Quantitative proteomic analysis reveals concurrent RNA–protein interactions and identifies  
672 new RNA-binding proteins in *Saccharomyces cerevisiae*. *Genome Res.* *23*, 1028–1038.

673 König, J., Zarnack, K., Rot, G., Curk, T., Kayikci, M., Zupan, B., Turner, D.J., Luscombe,  
674 N.M., and Ule, J. (2010). iCLIP reveals the function of hnRNP particles in splicing at  
675 individual nucleotide resolution. *Nat. Struct. Mol. Biol.* *17*, 909–915.

676 Kudla, G., Granneman, S., Hahn, D., Beggs, J.D., and Tollervey, D. (2011). Cross-linking,  
677 ligation, and sequencing of hybrids reveals RNA–RNA interactions in yeast. *Proc. Natl.*  
678 *Acad. Sci.* *108*, 10010–10015.

679 Lapointe, C.P., Wilinski, D., Saunders, H.A.J., and Wickens, M. (2015). Protein-RNA  
680 networks revealed through covalent RNA marks. *Nat. Methods* *12*, 1163–1170.

681 Lerner, M.R., and Steitz, J.A. (1979). Antibodies to small nuclear RNAs complexed with  
682 proteins are produced by patients with systemic lupus erythematosus. *Proc. Natl. Acad. Sci.*  
683 *U. S. A.* *76*, 5495–5499.

684 Licatalosi, D.D., Mele, A., Fak, J.J., Ule, J., Kayikci, M., Chi, S.W., Clark, T.A., Schweitzer,  
685 A.C., Blume, J.E., Wang, X., et al. (2008). HITS-CLIP yields genome-wide insights into  
686 brain alternative RNA processing. *Nature* *456*, 464–469.

687 Linder, B., Grozhik, A.V., Orlarin-George, A.O., Meydan, C., Mason, C.E., and Jaffrey,  
688 S.R. (2015). Single-nucleotide-resolution mapping of m6A and m6Am throughout the  
689 transcriptome. *Nat. Methods* 12, 767–772.

690 Maticzka, D., Ilik, I.A., Aktas, T., Backofen, R., and Akhtar, A. (2017). uvCLAP: a fast, non-  
691 radioactive method to identify in vivo targets of RNA-binding proteins. *BioRxiv* doi:  
692 10.1101/158410.

693 McMahon, A.C., Rahman, R., Jin, H., Shen, J.L., Fieldsend, A., Luo, W., and Rosbash, M.  
694 (2016). TRIBE: Hijacking an RNA-Editing Enzyme to Identify Cell-Specific Targets of  
695 RNA-Binding Proteins. *Cell* 165, 742–753.

696 Mili, S., and Steitz, J.A. (2004). Evidence for reassociation of RNA-binding proteins after  
697 cell lysis: Implications for the interpretation of immunoprecipitation analyses. *RNA* 10,  
698 1692–1694.

699 Moore, M.J., Zhang, C., Gantman, E.C., Mele, A., Darnell, J.C., and Darnell, R.B. (2014).  
700 Mapping Argonaute and conventional RNA-binding protein interactions with RNA at single-  
701 nucleotide resolution using HITS-CLIP and CIMS analysis. *Nat. Protoc.* 9, 263–293.

702 Nicholson, C.O., Friedersdorf, M., and Keene, J.D. (2017). Quantifying RNA binding sites  
703 transcriptome-wide using DO-RIP-seq. *RNA* 23, 32–46.

704 Niranjankumari, S., Lasda, E., Brazas, R., and Garcia-Blanco, M.A. (2002). Reversible  
705 cross-linking combined with immunoprecipitation to study RNA–protein interactions in vivo.  
706 *Methods* 26, 182–190.

707 Nues, R. van, Schweikert, G., Leau, E. de, Selega, A., Langford, A., Franklin, R., Iosub, I.,  
708 Wadsworth, P., Sanguinetti, G., and Granneman, S. (2017). Kinetic CRAC uncovers a role  
709 for Nab3 in determining gene expression profiles during stress. *Nat. Commun.* 8, 12.

710 Rogelj, B., Easton, L.E., Bogu, G.K., Stanton, L.W., Rot, G., Curk, T., Zupan, B., Sugimoto,  
711 Y., Modic, M., Haberman, N., et al. (2012). Widespread binding of FUS along nascent RNA  
712 regulates alternative splicing in the brain. *Sci. Rep.* 2, 603.

713 Rosenberg, M., Blum, R., Kesner, B., Maier, V.K., Szanto, A., and Lee, J.T. (2017).  
714 Denaturing CLIP, dCLIP, Pipeline Identifies Discrete RNA Footprints on Chromatin-  
715 Associated Proteins and Reveals that CBX7 Targets 3' UTRs to Regulate mRNA Expression.  
716 *Cell Syst.* 5, 368–385.e15.

717 Sanford, J.R., Coutinho, P., Hackett, J.A., Wang, X., Ranahan, W., and Caceres, J.F. (2008).  
718 Identification of Nuclear and Cytoplasmic mRNA Targets for the Shuttling Protein SF2/ASF.  
719 *PLoS ONE* 3, e3369.

720 Schor, I.E., Llères, D., Risso, G.J., Pawellek, A., Ule, J., Lamond, A.I., and Kornblihtt, A.R.  
721 (2012). Perturbation of Chromatin Structure Globally Affects Localization and Recruitment  
722 of Splicing Factors. *PLOS ONE* 7, e48084.

723 Shetlar, M.D., Carbone, J., Steady, E., and Hom, K. (1984). Photochemical Addition of  
724 Amino Acids and Peptides to Polyuridylic Acid. *Photochem. Photobiol.* 39, 141–144.

725 Silverman, I.M., Li, F., Alexander, A., Goff, L., Trapnell, C., Rinn, J.L., and Gregory, B.D.  
726 (2014). RNase-mediated protein footprint sequencing reveals protein-binding sites  
727 throughout the human transcriptome. *Genome Biol.* *15*, R3.

728 Singh, G., Ricci, E.P., and Moore, M.J. (2014). RIPit-Seq: A high-throughput approach for  
729 footprinting RNA:protein complexes. *Methods* *65*, 320–332.

730 Sugimoto, Y., König, J., Hussain, S., Zupan, B., Curk, T., Frye, M., and Ule, J. (2012).  
731 Analysis of CLIP and iCLIP methods for nucleotide-resolution studies of protein-RNA  
732 interactions. *Genome Biol* *13*, R67.

733 Sugimoto, Y., Vigilante, A., Darbo, E., Zirra, A., Militti, C., D’Ambrogio, A., Luscombe,  
734 N.M., and Ule, J. (2015). hiCLIP reveals the in vivo atlas of mRNA secondary structures  
735 recognized by Staufen 1. *Nature* *519*, 491–494.

736 Sugimoto, Y., Chakrabarti, A.M., Luscombe, N.M., and Ule, J. (2017). Using hiCLIP to  
737 identify RNA duplexes that interact with a specific RNA-binding protein. *Nat. Protoc.* *12*,  
738 611–637.

739 Tenenbaum, S.A., Carson, C.C., Lager, P.J., and Keene, J.D. (2000). Identifying mRNA  
740 subsets in messenger ribonucleoprotein complexes by using cDNA arrays. *Proc. Natl. Acad.*  
741 *Sci.* *97*, 14085–14090.

742 Ule, J., Jensen, K.B., Ruggiu, M., Mele, A., Ule, A., and Darnell, R.B. (2003). CLIP  
743 Identifies Nova-Regulated RNA Networks in the Brain. *Science* *302*, 1212–1215.

744 Ule, J., Jensen, K., Mele, A., and Darnell, R.B. (2005). CLIP: A method for identifying  
745 protein–RNA interaction sites in living cells. *Methods* *37*, 376–386.

746 Van Nostrand, E.L., Pratt, G.A., Shishkin, A.A., Gelboin-Burkhart, C., Fang, M.Y.,  
747 Sundararaman, B., Blue, S.M., Nguyen, T.B., Surka, C., Elkins, K., et al. (2016). Robust  
748 transcriptome-wide discovery of RNA-binding protein binding sites with enhanced CLIP  
749 (eCLIP). *Nat. Methods* *13*, 508–514.

750 Van Nostrand, E.L., Gelboin-Burkhart, C., Wang, R., Pratt, G.A., Blue, S.M., and Yeo, G.W.  
751 (2017a). CRISPR/Cas9-mediated integration enables TAG-eCLIP of endogenously tagged  
752 RNA binding proteins. *Methods* *118–119*, 50–59.

753 Van Nostrand, E.L., Nguyen, T.B., Gelboin-Burkhart, C., Wang, R., Blue, S.M., Pratt, G.A.,  
754 Louie, A.L., and Yeo, G.W. (2017b). Robust, Cost-Effective Profiling of RNA Binding  
755 Protein Targets with Single-end Enhanced Crosslinking and Immunoprecipitation (seCLIP).  
756 In *MRNA Processing*, Y. Shi, ed. (New York, NY: Springer New York), pp. 177–200.

757 Van Nostrand, E.L., Shishkin, A.A., Pratt, G.A., Nguyen, T.B., and Yeo, G.W. (2017c).  
758 Variation in single-nucleotide sensitivity of eCLIP derived from reverse transcription  
759 conditions. *Methods* *126*, 29–37.

760 Van Nostrand, E.L., Freese, P., Pratt, G.A., Wang, X., Wei, X., Blue, S.M., Dominguez, D.,  
761 Cody, N.A.L., Olson, S., Sundararaman, B., et al. (2017d). A Large-Scale Binding and  
762 Functional Map of Human RNA Binding Proteins. *BioRxiv* doi: 10.1101/179648.

763 Wang, Z., Kayikci, M., Briese, M., Zarnack, K., Luscombe, N.M., Rot, G., Zupan, B., Curk,  
764 T., and Ule, J. (2010). iCLIP Predicts the Dual Splicing Effects of TIA-RNA Interactions.  
765 PLOS Biol. 8, e1000530.

766 Weyn-Vanhenryck, S.M., Mele, A., Yan, Q., Sun, S., Farny, N., Zhang, Z., Xue, C.,  
767 Herre, M., Silver, P.A., Zhang, M.Q., et al. (2014). HITS-CLIP and Integrative Modeling  
768 Define the Rbfox Splicing-Regulatory Network Linked to Brain Development and Autism.  
769 Cell Rep. 6, 1139–1152.

770 Windhager, L., Bonfert, T., Burger, K., Ruzsics, Z., Krebs, S., Kaufmann, S., Malterer, G.,  
771 L'Hernault, A., Schilhabel, M., Schreiber, S., et al. (2012). Ultrashort and progressive 4sU-  
772 tagging reveals key characteristics of RNA processing at nucleotide resolution. Genome Res.  
773 22, 2031–2042.

774 Yeo, G.W., Coufal, N.G., Liang, T.Y., Peng, G.E., Fu, X.-D., and Gage, F.H. (2009). An  
775 RNA code for the FOX2 splicing regulator revealed by mapping RNA-protein interactions in  
776 stem cells. Nat. Struct. Mol. Biol. 16, 130–137.

777 Zarnegar, B.J., Flynn, R.A., Shen, Y., Do, B.T., Chang, H.Y., and Khavari, P.A. (2016).  
778 irCLIP platform for efficient characterization of protein-RNA interactions. Nat. Methods 13,  
779 489–492.

780 Zhang, C., and Darnell, R.B. (2011). Mapping in vivo protein-RNA interactions at single-  
781 nucleotide resolution from HITS-CLIP data. Nat. Biotechnol. 29, 607–614.

782 Zhao, J., Ohsumi, T.K., Kung, J.T., Ogawa, Y., Grau, D.J., Sarma, K., Song, J.J., Kingston,  
783 R.E., Borowsky, M., and Lee, J.T. (2010). Genome-wide Identification of Polycomb-  
784 Associated RNAs by RIP-seq. Mol. Cell 40, 939–953.

785



## 786 **Figure Legends**

787 *Figure 1: The core steps of iCLIP and other variants of CLIP.*

788 The majority of currently available CLIP protocols (18 out of 28, Table S1) amplify truncated  
789 cDNAs to identify the protein-RNA crosslink sites. Therefore, this schematic follows the core  
790 steps of iCLIP, a variant that was developed to amplify truncated cDNAs. The structure of  
791 RNA fragments, cDNA inserts, and sequenced reads is marked along with colour-coded  
792 adapters, unique molecular identifiers (UMI), experimental barcodes and primers. The  
793 adapters are named as SeqRv and SeqFw, according to their conventional orientations  
794 relative to the final sequenced reads. Where indicated, variations introduced by other CLIP  
795 protocols are illustrated.

796 *Table 1: List of CLIP and related protocols*

797 Protocols are ordered by the year of publication to reflect their historical development.  
798 Updated publications introducing important variations to the same method are grouped with  
799 the initial publication. Protocols that are not aimed at studying the specificity of an RBP, but  
800 that apply the CLIP technology to a new purpose, are listed at the end.

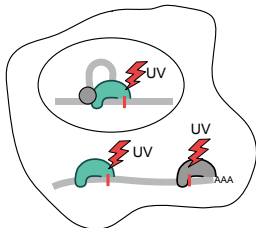
801 *Table 2: The core steps of CLIP and their variations*

802 The 11 core steps of the CLIP are listed, as well as the primary variations made in each step  
803 over the last 15 years, along with the names and publication dates of protocols that first  
804 introduced each variation. The number of CLIP protocols from the list in Table 1 and the  
805 number of developer labs that adopted each variant is shown, with the full list behind these  
806 numbers available in Table S1. A description and explanation of the rationale behind each  
807 variation is provided.

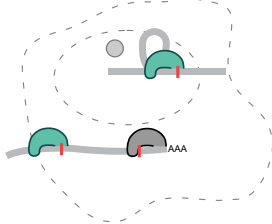
808 *Table S1. Related to Figure 1 and Table 2: Adopted variations in published CLIP protocols*

809 For all CLIP variants listed in Table 1, the variations adopted by each specific protocol are  
810 annotated. Boxes in black apply when none of the variants of the corresponding step are  
811 implemented by a protocol.

## 1. Covalent protein-RNA crosslinking



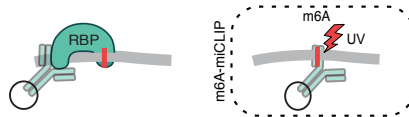
## 2. Cell lysis



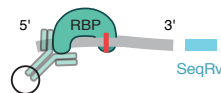
## 3. RNA fragmentation



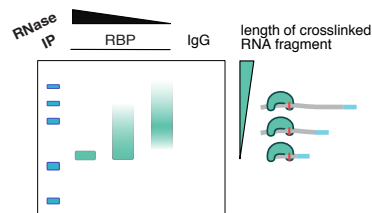
## 4. Purification of protein-RNA complexes



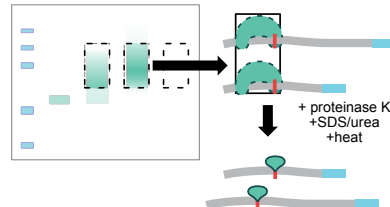
## 5. Ligation of SeqRv adapter to fragmented RNA



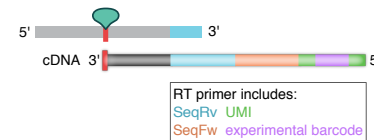
## 6. Quality control



## 7. RNA extraction

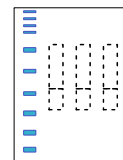


## 8. Reverse transcription



## 9. cDNA purification

## TBE-urea PAGE



optimal size of cDNA insert

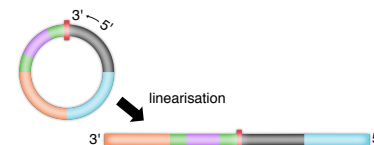
## Alternative strategies

Beads- or column-based purification:

- FAST-iCLIP
- BrdU CLIP
- irCLIP
- eCLIP
- FLASH
- sCLIP

## 10. SeqFw adapter ligation

intramolecular ligation (iCLIP and 15 derived protocols)



## 11. cDNA amplification and sequencing of multiplexed libraries

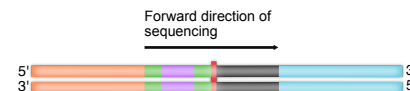


**Table1**

<b>Acronym</b>	<b>Full Name</b>	<b>Citation of Protocol</b>
CLIP and related protocols		
RIP	RNA immunoprecipitation	Lerner and Steitz, 1979
CLIP	(UV) Crosslinking and immunoprecipitation	Ule et al., 2003 Ule et al., 2005
Fractionation CLIP	CLIP from nucleus, cytosol and polysomes	Sanford et al., 2008
HITS-CLIP	High-throughput sequencing of RNA isolated by CLIP	Licatalosi et al., 2008 Chi et al., 2009
CLIP-seq	CLIP coupled with high-throughput sequencing	Yeo et al., 2009
CRAC	UV cross-linking and analysis of cDNAs	Granneman et al., 2009
PAR-CLIP	Photoactivable ribonucleoside-enhanced CLIP	Hafner et al., 2010 Garzia et al., 2017
iCLIP	Individual-nucleotide resolution CLIP	König et al., 2010
CLAP	Crosslinking and affinity purification	Wang et al., 2010
4SU-iCLIP	4SU-mediated crosslinking followed by iCLIP	Huppertz et al., 2014
urea-iCLIP	iCLIP with denaturing purification	Huppertz et al., 2014
BrdU CLIP	Bromodeoxyuridine UV CLIP	Weyn-Vanhenhenryck et al., 2014
FAST-iCLIP	Fully automated and standardized iCLIP	Flynn et al., 2015
irCLIP	Infrared-CLIP	Zarnegar et al., 2016
eCLIP	Enhanced CLIP	Van Nostrand et al., 2016
seCLIP	Single-end eCLIP	Van Nostrand et al., 2017c
uvCLAP	UV crosslinking and affinity purification	Aktaş et al., 2017
FLASH	Fast ligation of RNA after some sort of affinity purification for high-throughput sequencing	Aktaş et al., 2017
Fr-iCLIP	Fractionation iCLIP	Brugiolo et al., 2017
sCLIP	Simplified CLIP	Kargapolova et al., 2017
dCLIP	Denaturing CLIP	Rosenberg et al., 2017
Further applications of CLIP		
CLASH	Cross-linking, ligation, and sequencing of hybrids	Kudla et al., 2011
hiCLIP	RNA hybrid and iCLIP	Sugimoto et al., 2015
PAPERCLIP	Poly(A) binding protein-mediated miRNA 3' end retrieval by CLIP	Hwang et al., 2016
cTag-PAPERCLIP	"Conditionally" tagged-PAPERCLIP	Hwang et al., 2017
m5C-miCLIP	Cytosine-5 methylation iCLIP	Hussain et al., 2013
m6A-miCLIP	N6-methyladenosine iCLIP	Linder et al., 2015

Core steps and their variations in CLIP protocols	Number of protocols (developer labs)	First protocol developing the variation	Description and rationale for each step and its variations
<b>1. Covalent protein-RNA crosslinking</b>			
UV-C crosslinking of intact cells or tissues	23 (11)	CLIP (2003)	UV-C crosslinking (254nm) can be applied on any type of sample, including postmortem human tissues, and its efficiency is generally similar to the use of UV-A with 4SU.
UV-A crosslinking of cells after incubation with photoactivatable ribonucleosides	3 (2)	PAR-CLIP (2010)	UV-A crosslinking (365nm) requires preincubation of cells with 4SU or 6SG. It can lead to preferential identification of those protein-RNA contact sites that contain U or G, and long preincubation with 4SU or 6SG can lead to cellular stress (Huppertz et al., 2014). It increases efficiency for some RBPs, and is likely to be particularly valuable for studies of RBP interactions with nascent RNAs.
Mutation-induced crosslinking	1 (1)	m5C-miCLIP (2013)	This method employs a mutant RNA methylase, NSun2, which forms a covalent bond with its m5C methylated base.
In vitro UV-C crosslinking of antibody to purified RNA	1 (1)	m6A-miCLIP (2015)	RNAs are purified from cells and fragmented. The RNA fragments are then incubated with m6A specific antibody. Captured RNA fragments are crosslinked to the antibody with UV-C.
<b>2. Cell lysis</b>			
Total cell	25 (11)	CLIP (2003)	RBP is purified from total cellular lysate, which enables to simultaneously examine all types of RNAs bound by an RBP in all cellular compartments.
Fractionated cells	3 (3)	Fractionation CLIP (2008) fr-iCLIP (2017)	RBP is purified from cellular subcompartments. The basic approach is to fractionate crosslinked cells into nuclear and cytosol fractions, and here polysomes are studied in addition. Here, nucleoplasm and chromatin are studied in addition to cytosol.
<b>3. RNA fragmentation</b>			
RNase digestion in lysate	23 (10)	CLIP (2003)	RNA fragmentation in the lysate ensures that RNA-dependent RNP complexes dissociate before incubation with the beads, thus avoiding co-purification of additional RBPs.
Controlled RNA fragmentation by optimising limited RNase digestion	21 (9)	CLIP (2005)	The procedure for optimising limited RNase digestion is presented by using gel shift analysis of protein-RNA complexes separated by SDS-PAGE. This is important to A) Ensure that the final cDNAs are long enough to enable unique genomic mapping. B) Overdigestion introduces sequence constraints and biases due to preferred RNase cleavage patterns (Haberman et al., 2017). C) Avoid insufficient RNase digestion, which could keep larger RNPs intact, thus leading to co-purification of non-specific RBPs and RNAs.
Use of RNase I	12 (6)	iCLIP (2010)	Most RNases preferentially cleave after one or two specific nucleotides. RNase I is capable of cleaving at all nucleotides, and thus has less sequence specificity than other RNases. This minimises the sequence bias of RNA fragmentation, thus decreasing the sequence constraints at cDNA ends (Haberman et al., 2017).
On-bead RNase digestion	5 (4)	PAR-CLIP (2010) irCLIP (2016)	In addition to RNase digestion in lysate, a second round of RNase digestion is performed on beads. This leads protein-RNA complexes migrating as a sharp band on SDS-PAGE, indicative of RNA overdigestion that can lead to short reads which may not map uniquely to the genome. On-bead RNase digestion allows the use of nuclease S1, a less efficient enzyme that is not compatible with in-lysate digestion. Nuclease S1 leaves a 3'OH group on RNA fragments, which is convenient by avoiding the need for an additional phosphatase step. However, the on-beads digestion might be less efficient in dissociating large RNP complexes.
In vitro fragmentation of purified RNA	1 (1)	m6A-miCLIP (2015)	Purified RNAs are fragmented by zinc(III)-mediated RNA cleavage.
<b>4. Purification of protein-RNA complexes</b>			
Immunoprecipitation under mild conditions		RIP (1979)	RNA immunoprecipitation, in its original version, is performed without RNase, and under conditions that are mild enough to preserve protein binding to the RNA targets without any crosslinking. This serves to identify RNAs enriched in the immunoprecipitation, rather than to define the position of binding sites.
Immunoprecipitation under stringent conditions	21 (10)	CLIP (2003)	Stringent washing with high salt buffers and ionic detergents preserves only the crosslinked protein-RNA contacts, followed by SDS-PAGE and membrane transfer to further separate any remaining co-purified proteins that are of different MW. Nitrocellulose membrane does not bind well to nucleic acids, thus allowing to further remove any remaining free RNAs.
Denaturing purification with the use of epitope tags	6 (4)	CRAC (2009) CLAP (2010) urea-iCLIP (2014) uvCLAP (2017) dCLIP (2017)	Uses two-step affinity purification of tagged proteins in yeast under denaturing conditions to completely remove any interacting RBPs and free RNAs that are not crosslinked to the protein of interest. Like CRAC, but uses two-step affinity purification of tagged proteins in mammalian cells under denaturing conditions. Relies on 8xHis- and two Strep-tag II peptides. While ensuring specificity, the method requires expression of tagged proteins, which may not fully reflect the binding pattern of untagged endogenous proteins. Like CLAP, but using a 3xFlag-tag, such that the RBP is eluted after the first immunoprecipitation with denaturing conditions (eg. high SDS or urea and heat), which is then followed by a second immunoprecipitation. Like CLAP, but replacing the 8xHis- and Strep-tag with 3xFlag-tag and histidine-biotin-histidine-tagging. RBP is fused with a biotinylation tag, which enables it to be biotinylated in cell lines expressing the bacterial biotin ligase BirA. The RBP is then purified with streptavidin beads and subjected to multiple denaturing 8M urea and 2% SDS washes.
<b>5. Ligation of SeqRv adapter to fragmented RNA</b>			
Ligation to purified RNA	4 (3)	CLIP (2003)	In the original protocol, adapters are ligated to RNA after membrane transfer and digestion of the protein. This requires an additional gel purification to remove the adapter, which leads to some loss of RNA. This protocol can also be prone to amplifying non-specific bacterial or yeast RNAs that can be introduced as contaminants during PAGE or transfer of the protein-RNA complexes, and adapter-adaptor concatamer artefacts. The protocol can be of use in rare cases where on-bead ligation is inefficient.
On-bead ligation	23 (10)	CLIP (2005)	On-bead ligation allows removal of the adapter by washing the beads, and free adapters are further removed by SDS-PAGE and transfer. Thus no additional step is needed to remove the adapter. The on-beads ligation is efficient when used with magnetic beads, as long as the RNA fragments are >15nt and the relative volume of beads vs. ligation reaction is appropriate. Its efficiency needs to be tested when changing the type of beads used.

Barcoded seqRv adapter	4 (3)	eCLIP (2016), uvCLAP (2017)	Allows multiplexing of experiments immediately after IP, which can save time and reduce experimental variation between samples. However, this loses the capacity to examine the specificity of purified protein-RNA complexes during the membrane visualisation step. It also requires PE sequencing or long sequencing reads, in order to ensure that the full cDNA together with the barcode in the SeqRv adapter are sequenced.
Polyadenylation of purified RNAs	1 (1)	sCLIP (2017)	Instead of ligating SeqRv, the purified RNA fragments are polyadenylated, and the poly(A) tail is then used as the template for annealing the RT primer.
6. Quality control			
Visualisation of PAGE-separated protein-RNA complexes	24 (11)	CLIP (2003)	Allows visualisation and validation of the specificity of the protein-RNA complexes, to confirm absence of non-specific co-purified RBPs or RNAs, and to demonstrate that RNase conditions are well optimised. The original protocol used radioactive 5' end labelling of RNA fragments for this purpose.
Non-radioactive visualisation of protein-RNA complexes	2 (2)	irCLIP (2016)	Infrared signal is introduced via a dye-coupled SeqRv adapter, which allows visualisation of protein-RNA complexes without the use of radioactivity, while also monitoring ligation efficiency.
		sCLIP (2017)	An aliquot of the immunoprecipitation is labelled by conjugating biotin-ADP to the 3' end of the crosslinked RNAs. Subsequently this is visualised with streptavidin-HRP chemiluminescence.
7. RNA extraction			
Proteinase digestion	28 (13)	CLIP (2003)	Proteinase K (PK) is used to cleave the protein crosslinked to RNA under denaturing conditions. This releases the RNA into solution, along with a small peptide that remains on the RNA at the crosslink site.
Use of SDS buffer	5 (4)	CRAC (2009)	Both urea and SDS denature proteins and enhance PK activity, but urea can be unstable upon prolonged storage, and therefore SDS is proposed to be used instead.
8. Reverse transcription			
Conversion of RNA fragments into cDNAs	28 (13)	CLIP (2003)	A primer complementary to the SeqRv adapter is used to convert RNA fragments into cDNAs.
Introduction of experimental barcodes and unique molecular identifiers (UMIs) into cDNAs	15 (7)	iCLIP (2010)	UMIs (also referred to as random barcodes, or randomers) allow to quantify the number of unique cDNAs that map to the same position in the genome, thus differentiating them from PCR amplicons of the same cDNA molecule, taking full advantage of highthroughput sequencing to the quantify cross-linking at specific nucleotides.
9. cDNA purification			
Denaturing acrylamide gel purification of ligated RNAs	3 (2)	CLIP (2003)	This step has been used by protocols that ligated both seqRv and seqFw adapters to the purified RNA in order to remove the adapters. After RT-PCR, the cDNA undergoes further size selection.
TBE-Urea acrylamide gel	9 (4)	iCLIP (2010)	Excess RT primers are removed with gel purification, which also serves to select specific cDNA size ranges as an additional quality control. This is followed by ethanol precipitation. Under optimal conditions, recovery is ~90%, but the method requires some experience to avoid carrying over salts or any other reagents that could inhibit PCR.
BrdU capture	3 (1)	BrdU CLIP (2014)	Br-dUTP replaces dTTP in the reverse transcription reaction, enabling purification of cDNAs by two rounds of immunoprecipitation with an anti-BrdU antibody. During the second round, cDNAs are circularised and linearised as in iCLIP, and then eluted by heating.
Streptavidin beads purification of cDNA	2 (1)	Fast-iCLIP (2015)	Streptavidin purification of cDNA is enabled via biotinylated SeqRv that has been ligated to RNA, and remains attached to cDNAs. After circularisation, cDNA is eluted from the streptavidin beads and column purified. This increases the convenience and speed of the protocol. After PCR amplification, cDNAs are then size-selected with acrylamide gel.
		irCLIP (2016)	Similar to Fast-iCLIP, but after circularisation, cDNA is incubated with isopropanol and AMPure beads for further purification and size selection of cDNA.
Silane beads purification of cDNA	2 (1)	eCLIP (2016)	After enzymatic degradation of free RT primers with Exo-SAP, cDNA is purified with silane beads, and after PCR amplification, further purified with native agarose gel.
Column purification of cDNA	2 (2)	FLASH (2017)	After RT, cDNA is column purified. There are no further purification steps after circularisation.
		sCLIP (2017)	After RT, the protocol employs second strand cDNA synthesis, <i>in vitro</i> transcription, and adapter ligation to the antisense RNA, each coupled with column-based purification steps.
10. SeqFw adapter ligation			
SeqFw adapter is ligated to the 5' end of RNA fragments	9 (5)	CLIP (2003)	SeqFw adapter is required to amplify cDNAs. Since it is ligated to the 5' ends of RNA fragments, the full RNA fragment needs to be reverse transcribed in order to create amplifiable cDNAs in CLIP. Therefore, only cDNAs that read through the crosslinked nucleotide can be amplified by PCR, leading to loss of truncated cDNAs.
SeqFw adapter is ligated to 3' end of cDNAs to enable amplification of truncated cDNAs	18 (8)	iCLIP (2010)	Ligation of SeqFw to cDNA is achieved by introducing the seqFw sequence into cDNAs via the RT primer, followed by its efficient intramolecular ligation to the 3' end of cDNAs with the use of circRigase. The circular cDNA is then linearised through a BamHI site in the RT primer, which then enables amplification and sequencing of both 'read-through' and 'truncated' cDNAs. When combined with analysis of clustered cDNA starts, this allows to map the position of the high-occupancy cross-linking with nucleotide resolution.
		Fast-iCLIP (2015)	As iCLIP, except that RT primer contains two carbon spacers between the SeqFw and SeqRv sequences, which allow termination of the PCR enzyme, thus removing the need for BamHI digestion.
		eCLIP (2016)	The cDNA circularisation is replaced by an intermolecular ligation of SeqFw with the use of RNA ligase.
11. cDNA amplification and sequencing of multiplexed libraries			
cDNA cloning and Sanger sequencing	4 (3)	CLIP (2003)	Individual cDNAs are cloned for Sanger sequencing.
High-throughput sequencing of multiplexed cDNA libraries	25 (12)	HITS-CLIP (2008)	Overhangs are added to PCR primers, which include experimental barcodes for each sample and sequencing adapters, which allows multiplexing of the cDNA libraries and high-throughput sequencing.
		Fast-iCLIP (2015)	Phusion enzyme is used for PCR, and qPCR is used to determine the optimal number of PCR cycles.